LHCP 2021

Tests of LM2 MicroMegas Modules on Cosmic Stand in Dubna

Mikhail Demichev, on behalf of Muon ATLAS Collaboration

Cosmic Stand in JINR (Dubna)

Introduction:

• The upgrade of Muon Spectrometer of ATLAS detector is driven by increased luminosity than will be delivered after LHC Upgrade. The inner endcap part of MS, the so called 'Small Wheel', is subjected to highest particle rate during collisions which will further increase at high luminosity LHC.
• New Small Wheel consists of 4 layers of fast trigger and tracking detectors the sTGC and precision coordinate tracker detectors the MicroMegas (microstrip and mesh gaseous detectors)
• New Small Wheel is divided into 16 smaller and 16 larger sectors. For MM production each sector is divided into inner part SM1, LM1 and outer part SM2, LM2. Last type of MM module is produced in cooperation between JINR(RF,Dubna) and AUoT(Greece) groups.

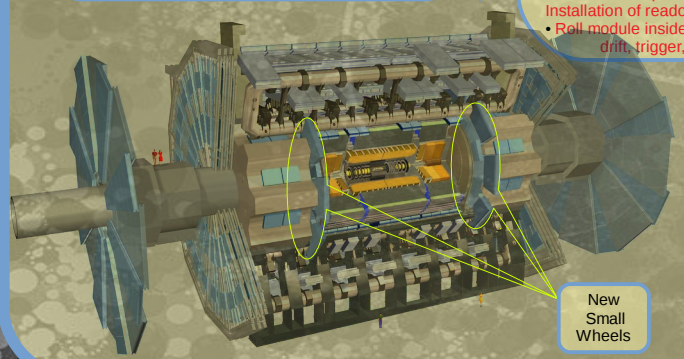

New Small Wheels

LM2 Modules Production and Tests:

• Drift panels with mesh under tension come from AUoT(Greece).
• Both sides of readout panels consist of industrially manufactured PCBs with signal strips, resistive strips and pillars to support the mesh
• In Dubna in controlled environment room PCBs of one side are aligned and fixed on vacuum tables, glued with mainframe and with other side.
• In a clean room LM2 module is assembled from 3 drift and 2 readout panels, undergoes gas tightness, alignment, and high voltage tests on dry air ~1kV and gas mixture of Ar and CO_2(93:7) at ~580V
• Module is prepared for Cosmic Stand test. Compression bars are installed. Electronic readout installation is probed with „dummy" readout board.
• Module is put on the trolley of Cosmic Stand. Installation of readout boards and connection tests.
• Roll module inside Cosmic Stand. Set up gas, LV, HV, drift, trigger, veto, ventilation, monitoring.

Assembled MicroMegas Module

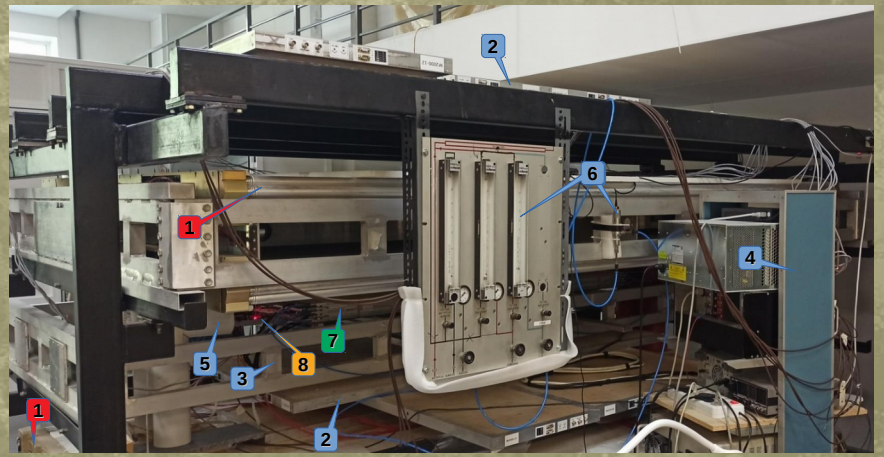

A general purpose Cosmic Test Stand in DLNP JINR

1. Two MDT chambers produced in 2005 for ATLAS MS – currently not used
2. Three scintillator counters on the top covering area 2.0x1.0m and similar counters at the bottom together with NIM logic units provide coincidence trigger for MicroMegas readout boards
3. Trolley on rails to put module under test inside Cosmic Stand
4. Inside the rack: Low Voltage and High Voltage power supplies, 1Gbit Ethernet switch, UPS, NIM logic, analogue and digital delay lines
5. Cooling vents with deflectors for readout boards, 6x25W
6. Gas flow indicator and absolute humidity sensor on the gas line exiting the module under test
7. Module LM2 is being tested
8. MMFE8 readout boards each has 8x64 channel VMM3 chips: charge amplifier + ADC + TDC in each channel. Having total of 14 R/O boards (just 8 in 2019) is enough to populate ½ LM2 module so installation is done twice (3 times in 2019) per module. All R/O boards were of limited pre-production series thus being a non-renewable resource.

Installation Method of MMFE8 Readout Boards

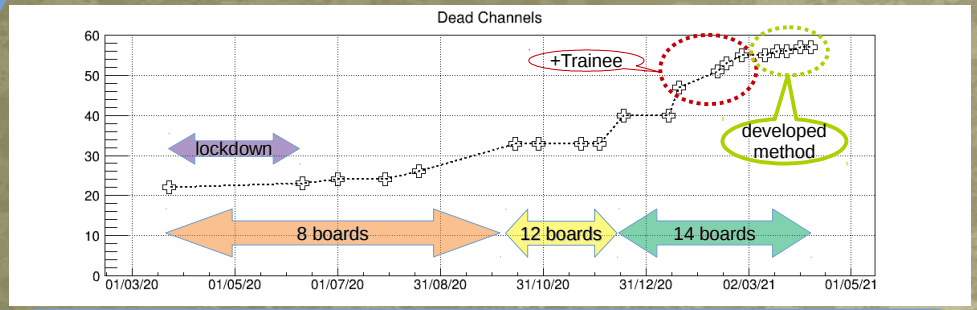

Correct installation of readout boards is quite a time-consuming enterprise. To establish contact between readout strips and board channels an elastic band with conductive micro-wires is used, so-called 'zebra' connector. Board is pressed against RO panel with cams of compression bar. In order not to damage the board the torque applied should not exceed 25 N·cm. This does not ensure good contact which is checked taking noise calibration runs. When several iterations of locking cams, changing and cleaning zebras or compression bars do not improve connection newcomers are tempted to override the torque limitation. This results in MMFE8 board deformations causing permanent damage to input channels. A new method is based on measuring the clearance between CB and detector plane using gauge bars and foils. Then CB should be aligned parallel to detector plane. Also MMFE8 board must be fastened with plastic clamp on its outer edge. Extra clearance measurements are done at the edge of the board to select a proper type of fastening kit and spacers and to ensure that locking the board gives no additional deformation which would affect contact quality and board lifespan. Together this give a reproducible installation technique.

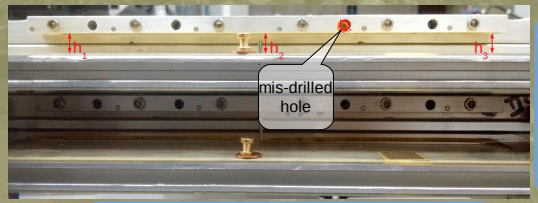

Compression Bar leveling:
If the clearance is less than 9.5mm, compression bar is loosened and a caliber bar of 9.5 mm is inserted between CB and detector plane for full length. If one of the clearances is > 0.1 mm smaller than the others, the caliber bar is inserted at this place with one end using spacers if required. If the reason for CB deformation is the misplacement of holes then short-threaded screws should be used. Finally the CB is fastened, the caliber bar is removed and measurement is repeated. This can be done at preparation step for Cosmic Stand testing.

Locking R/O Board Free Edge:
The CB pillar together has a typical height of 5.5 mm and D=4mm copper washer 0.80 – 0.85 mm. If clearance between R/O board and detector plane is less than 6.3 mm a flattened washer can be used up to 0.2 mm height. If the clearance in the range [6.3, 6.9] mm, the gap can be filled with tiny spacers made from copper 0.2mm foil. A plastic clamp is elastic enough so than up to 3 such spacers can be used. Otherwise D=2.5x15mm screw with D=5.0x6.5mm bushing should be used. Extra copper washers of different height could be used as spacers. Clearance measurement is repeated after locking readout board free edge.

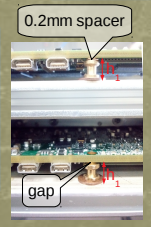

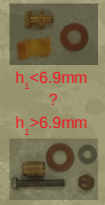

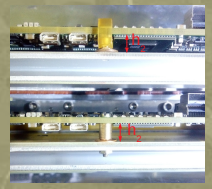

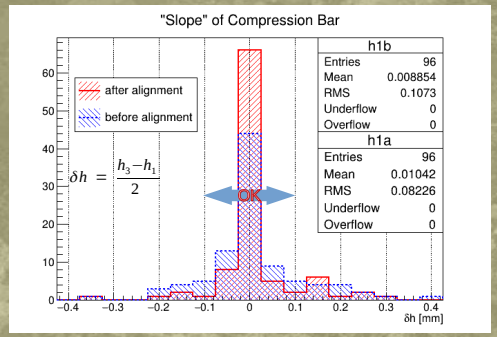

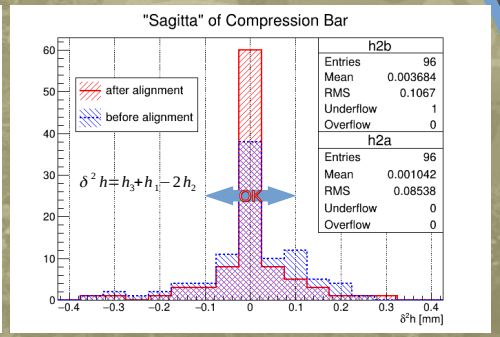

As the result of CB leveling dispersion of CB slope and sagging decreases. Some of CBs resist alignment due to precision pins shift. It is desirable that all 6 cams of CB lock at the same facet at applied required torque of 25 N·cm, one facet step is 0.2mm. Also CB cam springs should be checked for permanent deformation and promptly replaced

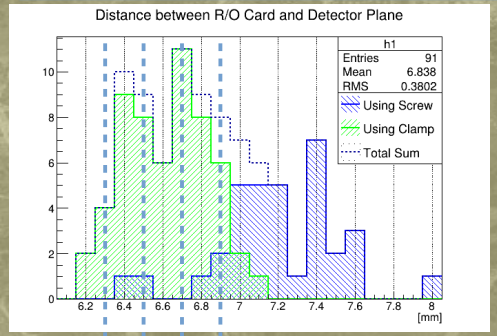

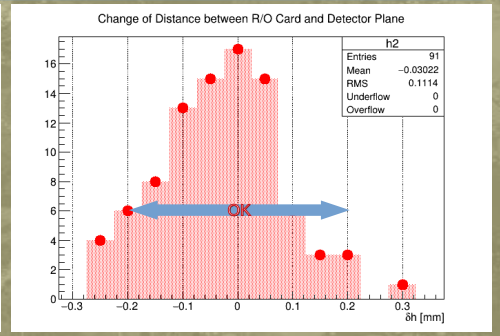

Clamp Pillar and D4 Washer h_0 = 6.3mm

+1 +2 +3

h_0 + N spacers 2x2x0.2 mm copper foil

Using D=2.5mm Screw and dedicated bushing is preferred

While the inner edge of R/O card is already locked by compression bar and outer edge is free, the distance from detector plane to card is measured at the center of card. Then near edge is either locked by clamp or fastened by screw with bushing and the distance is measured second time. It is OK to continue if the difference falls within 0.2 mm tolerance.
This method preserves R/O cards from deformations providing contact with strips and mechanical stability.

Module Efficiency and Cluster Charge Maps

Efficiency measurement

The track reconstruction algorithm starts with building clusters from consequent hits in one layer with a single strip gap allowed for a cluster. A weighted average is taken to find cluster centroid where hit weight is a charge collected on a strip. Precision coordinate Y is across the strips, auxiliary coordinate X is along eta strips and Z is perpendicular to detector plane. Having 2 clusters in eta strips is enough to restore polar angle of track in YZ plane. As stereo strips 3,4 are rotated with respect to eta strips 1,2 by 1.5° in opposite directions the actual strip hit by a track will vary with by ΔY ~ X coordinate. Simplify calculations by ignoring the change of X coordinate with Z inside the module (actual X resolution is too low).

$$\begin{cases} Y_{S3} = Y_{E1} + 2(Y_{E2} - Y_{E1}) + \Delta Y \\ Y_{S4} = Y_{E1} + 3(Y_{E2} - Y_{E1}) - \Delta Y \end{cases}$$

$$where \quad \Delta Y = X\frac{\tan(\alpha)}{pitch} \approx 0.0582 \cdot X$$

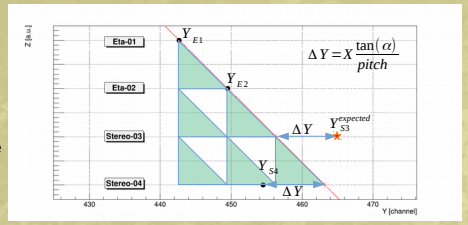

Given Y-coordinates of cluster centers in three reference layers (closed circles) we can rewrite this system of equations to calculate the expected Y hit position (star) in the fourth test layer altogether with X-coordinate.

$$Y_{E1}^{expected} = 1/3(5Y_{E2} - Y_{S3} - Y_{S4}), \quad X = 1/3(Y_{E2} - 2Y_{S3} + Y_{S4})\frac{pitch}{\tan(\alpha)}$$

$$Y_{E2}^{expected} = 1/5(3Y_{E1} + Y_{S3} + Y_{S4}), \quad X = 1/5(Y_{E1} - 3Y_{S3} + 2Y_{S4})\frac{pitch}{\tan(\alpha)}$$

$$Y_{S3}^{expected} = -3Y_{E1} + 5Y_{E2} - Y_{S4}, \quad X = (2Y_{E1} - 3Y_{E2} + Y_{S4})\frac{pitch}{\tan(\alpha)}$$

$$Y_{S4}^{expected} = -3Y_{E1} + 5Y_{E2} - Y_{S3}, \quad X = (Y_{E1} - 2Y_{E2} + Y_{S3})\frac{pitch}{\tan(\alpha)}$$

If there is a real cluster in the layer of interest in proximity of expected position then N_{eff}[Y,X] counter is increased otherwise N_{ineff}[Y,X] counter is increased. Finally efficiency is calculated as

$$\epsilon = \frac{N_{eff}}{N_{eff} + N_{ineff}}$$

In actual measurement the probe track is reconstructed from clusters preselected by high charge and shortened arrival time window to reject fake tracks. Contrary to this the cluster in the layer of interest has no selection. However charge distribution of such 'pointed' clusters and their arrival time is monitored.

Collected cluster charge distribution in every [Y,X] bin is fitted with Landau p.d.f. The map of fitted function MPV parameter is drawn in addition to efficiency map. This provides extra information about gas charge amplification non-uniformity which is not observable in the areas with too high or too low efficiency.

While having just two clusters in two different layers provides track angle information in YZ plane and even gives a crude estimate of efficiency distribution along Y it cannot restore X-coordinate. Smaller areas of inefficiency in one layer due to broken strips or applied passivation appear as 'ghost' areas with low statistics in three other layers. Module edges where stereo strips diverge and not cover fully etas area also cannot be measured.

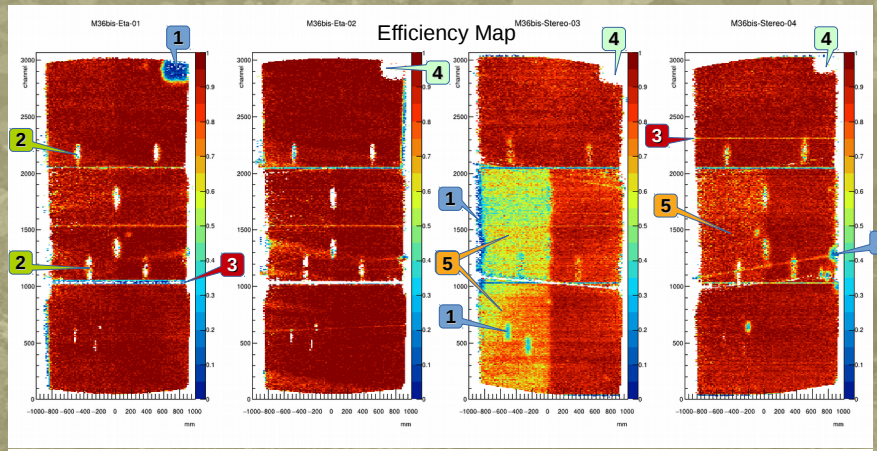

1. Areas of observed discharges were passivated by Araldite or Polyurethane glue
2. Interconnections – mechanic insertions for module rigidity and gas exchange
3. Artifacts of signal strips, shortcuts or cutoffs
4. 'Ghost' areas with low statistics due to inefficiency in one of three other layers
5. High voltage sectors with reduced potential, 550V for ST-03 and 570V for ET-01 and ST-04

Cluster charge on the colored palette of Z-axis is in fC

Atmospheric Pressure Effects

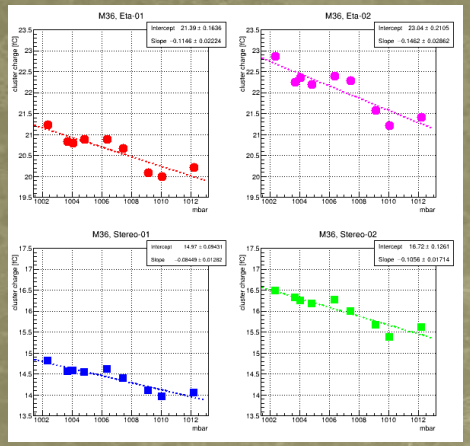

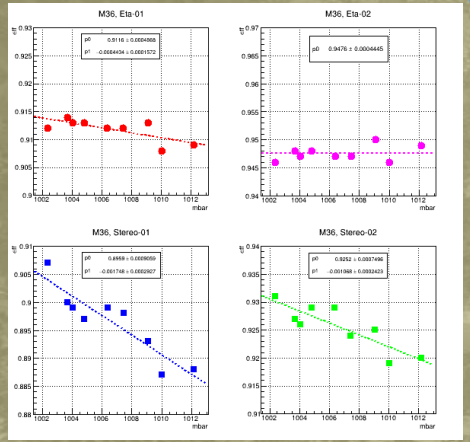

• MicroMegas modules operate at atmospheric pressure with constant overpressure ~1 mbar to provide continuous gas flow. Gas gain depends on the electron mean free path so variations of measured signal amplitude with atmospheric pressure are expected and observed.
• Efficiency drop with pressure is observed on the level of 0.0 ÷ 0.2 % / mbar
• Elevation above sea level in Dubna is 125m while in CERN at BB5 is 420m. This gives average pressure drop from Dubna to CERN about 33 mbar. To partially compensate for possible drop in efficiency cosmic tests in Dubna were done with increased high voltage +10V to nominal. So in terms of gas sparking modules have successfully passed tests in even more extreme conditions than in CERN.

Voltage Dependence

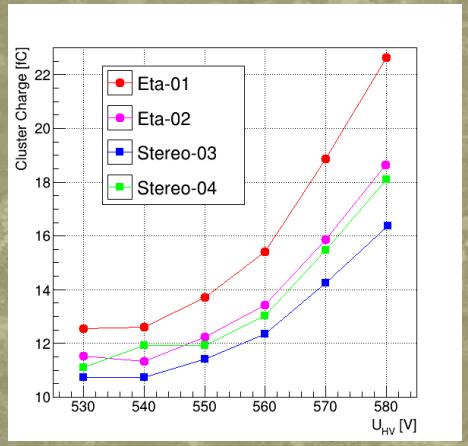

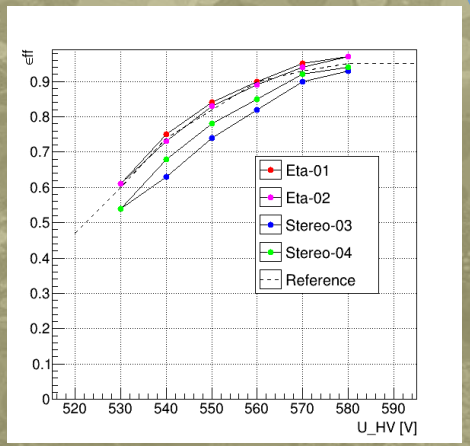

• Signal amplitude is expected to have nearly exponential increase with high voltage
• Efficiency of a good layer is expected to increase with high voltage and then saturate around ~ 90-98%
• Reference curve was measured for Module-0 at CERN, atmospheric pressure conditions might be different

Conclusions:

• 33 LM2 modules were assembled and tested in JINR (Dubna) for ATLAS NSW Upgrade. Some of them were repaired then re-assembled again so that passed cosmic tests twice.
• For each layer of each module 2D maps of efficiency and cluster charge distributions have been produced.
• Effect of atmospheric pressure changes is observed
• Each readout board was installed and removed O(100) times. Great experience in careful board installation was gained over time. However this experience was personal and is not readily transferable to colleagues. An installation method based on clearance measurements was developed giving repeatable results with only minor expert interventions. All of the 14 boards used for measurements remain operational.

Acknowledgements:

The author thanks all members of Dubna LM2 construction team for great experience and pleasure of working together: Balyikina M., Buadze B., Chubinidze Z., Gongadze Alexi, Gongadze I., Gongadze L., Dedovich D., Doroshkevitch N., Kaurtzev N., Kovyazina N., Khartchenko D., Minashvili I.jr., Potrap I., Rudenko T., Sotensky R.